

1 **Optimum three-point linkage set up for improving the quality of soil spectra**
2 **and the accuracy of soil phosphorus measured using an on-line visible and**
3 **near infrared sensor**
4

5 A. M. Mouazen^a, M. R. Maleki^{b, c}, L. Cockx^d, M. Van Meirvenne^d, L. H. J. Van Holm^e, R.
6 Merckx^e, J. De Baerdemaeker^b, H. Ramon^b

7
8 ^a *Natural Resources Department, Cranfield University, MK43 OAL, United Kingdom, e-mail:*
9 *a.mouazen@cranfield.ac.uk, Tel.: +44 1234 750111, Fax: +44 1234 752 971*

10 ^b *Division of Mechatronics, Biostatistics and Sensors (MeBioS), Department of Biosystems, Faculty of Bioscience*
11 *Engineering, Kasteelpark Arenberg 30, B-3001 Heverlee, Belgium*

12 ^c *Department of Agricultural Machinery, College of Agriculture, Shahid Bahonar University of Kerman, P.O. Box*
13 *76169-133, Kerman, Iran*

14 ^d *Research Group Soil Spatial Inventory Techniques, Department of Soil Management and Soil Care, Ghent*
15 *University, Coupure 653, 9000 Gent, Belgium*

16 ^e *Division of Soil and Water Management, Laboratory of Soil and Water Management, Faculty of Bioscience*
17 *Engineering, Kasteelpark Arenberg 20, B-3001 Heverlee, Belgium*

18
19 **Abstract**

20
21 On-line measurement of soil properties using the visible (Vis) and near infrared (NIR)
22 spectroscopy is sensitive to soil-to-sensor distance (D) and angle (α) variations, which have
23 prevented the successful development of on-line soil sensors so far. This study was undertaken
24 to minimise these variations through optimising the three-point linkage of the tractor to improve
25 the quality of soil spectra and the accuracy of plant available phosphorus (P-av1) measured with
26 an on-line soil sensor. The sensor consisted of a tine, to the back of which an optical probe was
27 attached to acquire soil spectra in diffusive reflectance mode from the bottom of the trench
28 opened by the tine. A mobile, fibre-type, Vis-NIR spectrophotometer (Zeiss Corona 45 visnir
29 fibre, Germany), with a measurement range of 306.5 – 1710.9 nm was used. Five lengths of the
30 third point link (L) of the tractor of 545, 550, 555, 560 and 565 mm were selected to evaluate
31 the quality of spectra collected on-line at 0.15 m tine depth. The on-line measured spectra were
32 corrected to remove the effect of D and α . The correction was evaluated by estimating the

33 accuracy of predicting P-avl using on-line measured spectra and a previously developed P-avl
34 calibration model.

35 Results showed that the best quality of spectra measured on-line was obtained for L of 555
36 mm, at which D and α vanished. This finding was supported by the maximum value of average
37 maximum reflectance (AMR) of 75.7% obtained and by 100% successfully collected spectra.
38 The worst quality of spectra was obtained at L of 545 mm, with the largest D of 6 mm and the
39 largest α of 0.6°. Values of L of 560 and 565 mm led to a decrease in the AMR (43.3 and
40 33.2%, respectively), while recording 100% successful spectra. Correction of on-line measured
41 spectra led to clear improvements in the accuracy of on-line measured P-avl. A lower root mean
42 square error (RMSE) of 1.07 mg 100g⁻¹ and higher ratio of prediction deviations (RPD) of 1.42
43 were obtained with corrected spectra as compared to uncorrected spectra (RMSE = 1.15 and
44 RPD = 1.39). In addition, the correction of spectra resulted in an increase in the degree of
45 similarity between laboratory and on-line measured P-avl maps by 29.6%. These results suggest
46 the need for optimising the tractor hydraulic three-point linkage set up, and for spectra
47 correction in order to improve the accuracy of on-line measured soil properties.

48

49 Keywords: visible; near infrared; spectrophotometer; on-line, soil sensor.

50

51 1. Introduction

52

53 Visible (Vis) and near infrared (NIR) diffusive reflectance spectroscopy is a promising
54 measurement technique available to provide rapid information about soil physical and chemical
55 properties, e.g. moisture, carbon, nitrogen, phosphorus and calcium content; and cation

56 exchange capacity in an economical manner (Ben-Dor and Banin, 1995; Chang *et al.*, 2001;
57 Reeves and McCarty 2001; Odlare *et al.*, 2005; Cozzolino and Morón, 2006; Maleki *et al.*,
58 2006a; Wetterlind *et al.*, 2008). When light is illuminated towards the soil surface, the radiant
59 energy is distributed through three different processes: reflection, absorbance and transmission
60 (Dahm and Dahm, 2001). Since transmission for opaque materials such as soils equals zero, the
61 balance between reflection and absorbance is governed by the influence of soil physical and
62 chemical properties (Mouazen *et al.*, 2005). The Vis-NIR spectroscopy was adopted by many
63 research groups to measure soil properties. Although several researchers reported off-line non-
64 mobile measurement of soil properties, only few studies on on-line measurement of soil
65 properties were reported (Shonk *et al.*, 1991; Sudduth and Hummel, 1993; Shibusawa *et al.*,
66 2003; Mouazen *et al.*, 2005). This is attributed to difficulties in designing a sensor that can
67 penetrate the soil and acquire spectra successfully (Mouazen *et al.*, 2007). In addition, lower
68 accuracy associated with providing general calibration models valid over a wide geographical
69 area enhances limiting the attraction of researchers to develop a working on-line sensor.
70 However, research is required to improve the performance of the few on-line Vis-NIR sensors
71 exist, since on-line data acquisition about soil is useful input for sensor-based variable rate
72 application of different inputs into agricultural soils (Maleki *et al.*, 2007).

73 Based on laboratory measurement of soil spectra using a Vis-NIR spectrophotometer, we
74 found the diffusive light reflected from the soil surface decreases with the increasing soil-to-
75 sensor distance (D) and angle between the soil and sensor (α). These two parameters induce
76 undesired changes in spectra, which requires a correction algorithm to retain the original
77 spectral features. Other researchers encountered the same problem during the development of
78 on-line measurement systems of soil properties (Sudduth and Hummel, 1993; Shibusawa *et al.*,

79 2003). Generally, D affects the accuracy of prediction of soil properties e.g. carbon, nitrogen,
80 etc (Sudduth and Hummel, 1993). Mouazen *et al.* (2005) claimed that they were able to
81 minimise D variation by introducing reasonably similar maps of moisture content developed by
82 an on-line sensor and oven drying method. In fact, the highest light reflection from the soil
83 surface can be recorded when direct contact between the soil and the sensor ($D = 0$ mm and $\alpha =$
84 0°) is ensured. During on-line measurement of soil properties the direct contact should be
85 fulfilled, bearing in mind that vibration can always exist during measurement that might disturb
86 the collection of spectra. However, the vibration induced noise can be eliminated from the
87 spectra by spectra pre-processing such as smoothing, normalisation and/or multiplicative
88 scatter correction (Mouazen *et al.*, 2005).

89 In order to keep the sensor in continuous contact with the soil, two conditions have to be
90 taken into consideration. Firstly, a proper mechanical design of the optical probe (the unit that
91 penetrates the soil and collects soil spectra) has to be provided, which should ensure continuous
92 penetration of the soil, preparation of a smooth soil surface and preservation of direct contact
93 between the soil and the optical probe (Mouazen *et al.*, 2005; Mouazen *et al.*, 2007). The other
94 condition is to ensure a proper calibration of the tractor three-point linkage, in order to attain
95 transactional and longitudinal levelling of the optical probe. This has to be accompanied with
96 manual adjustment of the tractor hydraulic system to locate the sensor to the required depth,
97 while preserving levelling of the sensor.

98 The main objective of this study was to develop a methodology to optimise the tractor three-
99 point linkage system set up, aiming at minimising D and α and improving the quality of on-line
100 collected soil spectra. The second aim of this study was to evaluate the effect of correction of

101 on-line measured spectra on the accuracy of prediction of plant available phosphorus in soil (P-
102 avl).

103

104 **2. Materials and methods**

105

106 *2.1. Portable, fibre-type visible and near infrared spectrophotometer*

107

108 The spectrophotometer was a fibre-type Vis-NIR instrument developed by Zeiss Company
109 (Zeiss Corona 45 visnir fibre, Germany). It is fast (1 soil scan per 0.4 sec) and of small size, has
110 no moving parts, and has been successfully used on mobile machines e.g. to measure grain
111 quality on combines (Reyns *et al.*, 2001; Maertens *et al.*, 2004), soil moisture content (Mouazen
112 *et al.*, 2005) and extractable P, P-avl, total carbon, organic carbon and pH (Mouazen *et al.*,
113 2007). It was also used to optimise an on-line variable rate applicator of triple super phosphate
114 (P_2O_5) during maize planting based on on-line measurement of soil extractable phosphorus
115 using the on-line Vis-NIR sensor of this study, shown in Fig. 1 (Maleki *et al.*, 2006b; Maleki *et*
116 *al.*, 2007). The instrument has, in addition to the Si-array available for the measurement in the
117 Vis and short infrared wavelength region (306.5 – 1135.5 nm), an InGaAs diode-array for the
118 measurement in the NIR region (944.5 – 1710.9 nm). The light source is a 20 Watt tungsten
119 halogen lamp illuminating the targeted soil surface with a spot of 2-3 mm light through an optic
120 fibre. The illumination and reflectance fibres were positioned at a 45° angle in an optical probe
121 used to carry out reflectance measurement from the soil surface prepared by the tine (Fig. 2).
122 Standard white (75% reflectance) and black (7% reflectance) references were used.

123

124 *2.2. On-line visible and near infrared soil sensor*

125

126 The on-line measurement system consisted of a penetration tine (subsoiler), to which the
127 optical probe is attached (Fig. 1). The tine and optical probe were set on a frame, which was
128 mounted onto the three-point linkage of the tractor. It is a simple frame, which has a metal
129 wheel on each side to regulate the subsoiler depth. However, depth control is only done in the
130 downwards direction by the two wheels. The upwards movement of the tine due to tractor
131 driving over a higher spot than that of the sensor driven behind can not be controlled. The depth
132 (draught based) control system linked to the hydraulic system of the tractor had to be set at
133 minimum response to draught variation during the field test to reduce vibration and variation in
134 D and α . The tine penetrates the soil to any required depth between 5 and 40 cm, making a
135 trench, whose bottom is smoothed due to the downwards force acting on the tine. This
136 downwards force increases friction between the flat bottom of the tine and its retrofitted probe
137 with the soil, which improves smoothing of the bottom of the trench and maximises light
138 reflectance.

139

140 *2.3. Laboratory calibration of the measurement system*

141

142 A preliminary test was undertaken under laboratory conditions to set the three-point linkage
143 and the hydraulic system of the tractor in a proper position that would ensure the tine
144 penetration to a depth of 15 cm, while preserving the optical probe in a horizontal position
145 (angle α and $D = 0$ in Fig. 2a) parallel to the bottom of the trench opened by the subsoiler. The
146 horizontal probe levelling included longitudinal and transactional adjustments of the upper third

147 point link and lower two-point links, respectively. The experiment showed that the optimal L is
148 555 mm, for which a longitudinal (parallel to the direction of travel) levelling of the optical
149 probe was achieved. In order to insure this position of the optical probe, the hydraulic system of
150 the tractor was manually adjusted to a given level. This optimal calibration set up obtained
151 under laboratory conditions, including the three-point linkage and hydraulic system, was
152 adopted during the on-line field measurement.

153

154 *2.4. Field measurement*

155

156 *2.4.1. Evaluation of the effect of different third point link lengths on quality of spectra*

157

158 To verify the laboratory calibration of the three-point linkage hydraulic system, on-line
159 measurement of soil spectra was carried out on a Haplic Luvisol (FAO classification) field in
160 Heverlee, 30 km east of Brussels (Belgium). The field soil texture determined by wet sieving
161 and a hydrometer test was a silt loam (Table 1), according to the United States Department of
162 Agriculture (USDA) system of texture classification. The experiment was carried out in the
163 autumn of 2005 after harvesting sugar beet. The field was even, particularly the plot where the
164 test was carried out. The optical sensor was pulled through 5 parallel lines, 5 m apart along a 15
165 m distance parallel with the direction of the tramlines. Carrying out the measurement within a
166 relatively small area of the field minimised the effect of variable soil conditions and field
167 topography, which allowed information about the effect of L on the quality of spectra to be
168 extracted.

169 The system was driven at a travel speed of 1.5 – 2.0 km h⁻¹, setting the tine tip at a depth of
170 0.15 m. Each collected spectrum was an average of 5 successive spectra collected along a
171 distance of 1 – 1.50 m, depending on tractor speed. The averaged gravimetric moisture content
172 (d.b.) for all lines was at the field capacity (Table 2), ranging between 18.7 and 20.1 kg kg⁻¹.
173 Five different L of 545, 550, 555, 560 and 565 mm were adopted. Each length was used for
174 measurement of one individual line. After measurement of an individual line, L was changed for
175 the next measurement line. This variation in L provided different positions of the optical probe
176 as shown in Fig. 2. Since the variation of α and D are very small (scale of few degrees and
177 millimetres for α and D, respectively), it was not possible to measure them precisely during on-
178 line measurement. Therefore, they were calculated theoretically under laboratory conditions and
179 reported in Table 2.

180

181 2.4.2. *Correction of on-line collected soil spectra*

182

183 Due to a technical issue associated with the Vis-NIR spectrophotometer from Zeiss company
184 used in this study, spectral shifts towards the upper or the lower directions were recorded during
185 on-line measurement with most of measured spectra at all L (Fig. 3). The shift occurred at 970
186 nm, which might be attributed to vibration and/or different D and α between the background
187 (reference) measurement and soil measurement. Furthermore, this spectral shift could also be
188 due to a differential response between the two detectors used (400-969 nm and 970-1700 nm). A
189 simple test under non-mobile laboratory conditions confirmed that vibration has no effect on the
190 creation of this shift. In fact, vibration induced noise in spectra along the entire wavelength
191 range. Examining the effect of different D and α between white reference measurement (D=0

192 mm and $\alpha=0^\circ$) and real soil measurement ($D>0$ mm and $\alpha\neq 0^\circ$) proved that the presence of shift
193 in spectra is due to variable D and α . The size of this shift depends on the magnitude of D and
194 α .

195 Spectra correction was done by developing a custom built software using the LabView
196 programming language. This software was based on the assumption of shifting the lower spectra
197 segment (at 306 – 968 nm or 972 – 1700 nm) to match the higher part. This was done as
198 follows:

- 199 1. The difference in reflectance in % between 968 and 972 nm wavelengths was calculated.
- 200 2. If the reflectance at wavelength 968 nm was higher than that at 972 nm, the reflectance
201 difference was added to all wavelengths in the range of 972 – 1700 nm. While, if the
202 reflectance at wavelength 968 nm was lower than that at 972 nm, the reflectance
203 difference was added to all wavelengths in the range of 306 – 968 nm.

204

205 *2.4.3. Evaluation of the effect of soil-to-sensor distance and angle variations on the prediction*
206 *accuracy of plant available phosphorus in soil*

207

208 Previous on-line measurement data from 2004 was recalled to test the effect of spectra
209 correction on improving the accuracy of prediction of P-avl, as an example. Availability of
210 chemical and spectral data from the previous year (2004) allowed the correction approach
211 proposed during Heverlee field measurement in 2005 (see section 2.4.2.) to be tested. The
212 measurement in Heverlee field in 2005 concerned about mechanical calibration only, where no
213 chemical data were available. The correction approach will be tested by comparing the
214 prediction accuracy of P-avl before and after removing the shift in spectra.

215 The experimental field in 2004 was a Haplic Luvisol (FAO classification) grass field of 2 ha
216 area and was situated in Lovenjoel near Leuven, and had silt loam texture according to the
217 USDA soil classification (Table 1). The field had a slight slope and was free of tram lines. The
218 field was divided into a 6 by 10 m grid, as shown in Fig. 4. The optical sensor was pulled along
219 the longest directions of the field through 18 parallel lines each 6 m apart at a forward speed of
220 2-3 km h⁻¹, setting the tip at a 0.15 m depth. A total of 126 soil samples were collected mostly
221 from the 6 middle lines (Fig. 4) after sensor passed. Each sample was collected at the bottom of
222 the trench opened by the tine over a distance of 1 – 1.5 m. The samples were dried and sieved
223 with a 2 mm sieve, before P-av1 was measured using the Olsen method (Olsen *et al.*, 1954). A
224 sufficient amount of wet samples was used to estimate the moisture content by drying in an oven
225 at 105° for 24 h. The average field moisture content was at the field capacity. The results of soil
226 moisture content and P-av1 of these samples are presented in Tables 2 and 3, respectively.

227 A digital global positioning system, Trimble® AgDGPS 132 was used to locate the position of
228 soil spectra. The 126 on-line collected spectra with a location matching the location of the 126
229 soil samples collected for laboratory analysis of P-av1 were later separated from the data set and
230 used to predict P-av1 using the model described in a previous study (Maleki *et al.*, 2006a). This
231 model was established using the Partial Least Squares (PLS) analysis with a full cross validation
232 technique on 204 independent spectra of fresh soil samples collected from many fields in
233 Belgium having these texture classes of loamy sand, sandy loam and silt loam. Measurement of
234 spectra used for developing P-av1 model was done under laboratory non-mobile measurement
235 conditions. The results of the calibration model and the prediction of P-av1 of 126 off-line
236 recorded spectra under laboratory condition of soil samples collected in Lovenjoel field is
237 illustrated in Table 4 (Maleki *et al.*, 2006a). This model was used in this study to predict P-av1

238 using spectra collected on-line in Lovenjoel field. Maps of laboratory Olsen measured and on-
 239 line predicted P-avl using on-line recorded spectra were developed using geostatistical software
 240 (GSLIB). The algorithm used was ordinary kriging (Goovaerts, 1997), which requires the
 241 determination of a variogram model. The experimental variogram was obtained through:

242

$$243 \quad \gamma(\mathbf{h}) = \frac{1}{2N(\mathbf{h})} \sum_{\alpha=1}^{N(\mathbf{h})} \{z(\mathbf{x}_{\alpha} + \mathbf{h}) - z(\mathbf{x}_{\alpha})\}^2 \quad (1)$$

244

245 where $\gamma(\mathbf{h})$ is the variogram for a distance vector (lag) \mathbf{h} between observations $z(\mathbf{x}_{\alpha})$ and $z(\mathbf{x}_{\alpha} +$
 246 $\mathbf{h})$, and $N(\mathbf{h})$ is the number of pairs separated by \mathbf{h} . The experimental variogram data were
 247 modelled by considering the indicative goodness of fit provided by Variowin (Pannatier, 1996).
 248 In all cases a spherical model was found to be best:

249

$$250 \quad \gamma(h) = C_0 + C_1 \cdot \left(\frac{3h}{2a} - \frac{1}{2} \left(\frac{h}{a} \right)^3 \right) \quad \text{if } 0 < h \leq a \quad (2)$$

$$251 \quad \gamma(h) = C_0 + C_1 \quad \text{if } h > a \quad (3)$$

252

253 where C_0 is the nugget effect (Y-intercept), C_0+C_1 is the sill and a is the range. The interpolated
 254 map cell size was 1 m² with 200 rows and 80 columns.

255 To compare variogram models, they were standardised by: $\gamma(h)/(C_0 + C_1)$. In this way all
 256 variograms received a sill of one.

257

258 3. Results and discussion

259

260 *3.1. Evaluation of soil spectra collected on-line at different third point link length*

261

262 Figure 3 shows soil spectra collected on-line for 5 different experimental lines carried out
263 with 5 different L, reflecting 5 values of angle α and D (Table 2). A total of 8 spectra for each
264 measurement line collected along 15 m travel distance are shown in Fig. 3.

265 With L equals to 545 mm (line A), the quality of spectra is extremely bad. Apart from 8
266 spectra only one spectrum is a soil spectrum. However, two other spectra are successfully
267 measured by the first detector (306 – 945 nm), while no reflection features are captured in the
268 near infrared region of (946 – 1700 nm). This poor quality of spectra is attributed to the fact that
269 the sensor focal point falls above the soil surface due to the large D. In this case the incidence of
270 the path of illuminated light and the path of reflected light does not occur at the bottom of trench
271 soil. But, in order to have a maximum collection of electromagnetic energy from the soil
272 surface, the focal point should fall directly on the soil surface, at which D and α vanish. This
273 means that the incidence of the illuminated and reflected light should strictly occur on the soil
274 surface following the passage of the tine and optical probe coming closely behind. The shift in
275 spectra between the two detectors increases in size with increasing D and α , until no signal is
276 collected at the NIR range, similar to Fig. 3a. This case can be represented by the position of the
277 measurement system illustrated in Fig. 2b, where the tine inclines towards the forward direction
278 forming an angle α with the horizontal. In this case, D and α are too large (Table 2), for which
279 only a very small amount of diffuse reflected light from the trench bottom could be captured by
280 the probe and reached the detector. Capturing this small amount of light takes place only when
281 the path of illumination light partially met with the path of the reflected light on the soil of the
282 bottom of the trench.

283 To evaluate the successful capturing of the reflected light, the maximum reflectance (in
284 percentage) measured for each spectrum was considered. The average maximum reflectance
285 (AMR) of all 8 spectra is adopted and reported in Table 5. Indeed, a very small value of AMR
286 of 7.8% is found during the measurement through line A. This also proves that a very small
287 percentage of reflected light from the soil surface could be captured.

288 Increasing L to 550 mm (line B) decreases D and α (Table 2), and subsequently the quality
289 of collected soil spectra improved (Fig. 3b). This is reflected by the number of successfully
290 collected soil spectra and by the AMR (Table 5). However, the values of these two indicators
291 are still too small to declare a well-levelled position of the optical probe on the bottom of the
292 opened trench. This means that α and D during line B measurement are still relatively big
293 (Table 2), and the probe position is still similar to the case illustrated in Fig. 2b.

294 The best soil spectra are collected with L of 555 mm (Line C in Fig. 3c). This observation is
295 justified by the fact that AMR obtained for line C is the highest among the 5 experimental
296 setups (Table 5). This case can be illustrated by Fig. 2a, where the tine is at the optimal position
297 allowing the bottom of the optical probe to be in continuous contact with the trench bottom
298 opened by the penetration tine (α and D = 0). This position should result in a smoother soil
299 surface at the bottom of the opened trench, and thus maximum light is reflected. The maximum
300 reflection is attributed to the incidence of the illumination light and reflected light on the soil
301 surface prepared by the system (Fig. 2a). The maximum value of AMR obtained here indicates
302 that the signal-to-noise ratio is high, and is higher than the other 5 experimental lines. The
303 percentage of successfully measured spectra is 100%, and all measured spectra can be used for
304 predictions of soil chemical and physical properties.

305 With further increase in L to 560 (line D) and 565 mm (Line E), the quality of soil spectra
306 acquired degrades. In this case the incidence of the illuminated light and reflected light falls
307 below the reflection surface of the soil (Fig. 2c) leading to light collection from only the edge of
308 the illuminated soil spot. This is reflected by the decrease in AMR values for both lines (Table
309 5). However, the number of successfully collected spectra does not change (100% successful
310 spectra). The decrease in the AMR for these two lines would mean a decrease of the signal-to-
311 noise ratio, and eventually the prediction accuracy of soil properties might be influenced.
312 Comparing the spectra collected for each measurement line, it can be concluded that the best
313 quality of spectra is obtained with 555 mm L (zero values of D and α), as illustrated in Fig. 3.

314

315 *3.2. Correction of on-line measured spectra*

316

317 Although L of 555 mm was found to be the optimal length, at which D and α theoretically
318 vanish, shift still occurs at a wavelength of 970 nm for most measured spectra, which
319 emphasises the need for spectra correction at any selected L. The disturbed and hollowed soil
320 structure that resulted after sugar beet extraction in Heverlee field could introduce significant
321 variation in D and α , which would explain this shift (Fig. 3). However, in grass or after harvest
322 of cereal crops, the authors found less occurrence of this shift in spectra. In fact, variation in D
323 and α can only be minimised, but not be avoided. The correction of soil spectra adopted in this
324 study to eliminate this shift results in smooth spectra without a shift up or down. Figure 5 shows
325 corrected spectra of those measured at L of 555 mm (Fig. 3c). These spectra had to be subjected
326 to further pre-processing (normalisation, derivation, smoothing, etc) before it can be used for the

327 final prediction of soil properties. The type of spectra pre-processing depends on the type of
328 element to be quantified (Mouazen *et al.*, 2006).

329 In order to evaluate the usefulness of the correction made on spectra to remove the shift that
330 occurred at 969 – 970 nm wavelength, the on-line measured spectra (126 spectra) in Lovenjoel
331 field were used to predict P-av1 using spectra with and without shift (corrected spectra). The
332 predicted P-av1 values of 126 spectra were compared with the corresponding laboratory
333 reference measurement of soil samples collected from the same locations. There is a difference
334 in the prediction accuracy of P-av1 values between on-line measured soil spectra collected from
335 field without spectra correction (root mean square error (RMSE) = 1.15 mg 100g⁻¹ and ratio of
336 prediction deviations (RPD) = 1.39) compared to those predicted with corrected spectra (RMSE
337 = 1.07 mg 100g⁻¹ and RPD = 1.42). This difference indicates only small improvement in the
338 prediction accuracy obtained after correction of spectra, as shown in Table 6. These point-by-
339 point statistics however do not take the spatial structure of the data into account. Therefore,
340 standardised variograms were calculated and modelled by a spherical model of the 126
341 laboratory measurements, the uncorrected and the corrected P-av1 values (Fig. 6). It can clearly
342 be observed that the variogram of the corrected P-av1 approaches more the variogram of the
343 laboratory values compared to the uncorrected values, with both the nugget effect and the range
344 closer to the values of the variogram of the laboratory data. This indicates that the spatial
345 structure of P-av1 is better captured by the corrected predictions compared to the uncorrected.

346 The improvement of using corrected spectra to predict P-av1 can also be shown as a map
347 basis. By visually comparing Figs. 7a, 7b and 7c, similarities in the spatial patterns of P-av1 are
348 obvious. Similarity between categorical maps is usually quantified through a statistical kappa
349 (κ) value (Cohen, 1960), expressing proportionally how much better the results are compared to

350 a purely random classification. The larger κ , the more accurate the classification. To obtain
351 categorical maps of P-avl, all maps were classified into five classes based on the 0.2, 0.4, 0.6
352 and 0.8 quantiles of the interpolated laboratory measurements. The resulting maps are shown in
353 Fig. 8a, 8b and 8c. The κ value of comparing the laboratory classification with the uncorrected
354 P-avl is 0.428, whereas for the comparison with the corrected P-avl classification κ is 0.555.
355 According to Landis and Koch (1977), the strength of agreement between the laboratory
356 classification and both the classification of the corrected and the uncorrected P-avl was
357 considered to be moderate. Nevertheless, the improvement of using corrected spectra for P-avl
358 prediction results in an increase in map similarity of 29.6% (based on the κ values).

359 The accuracy of P-avl map developed in this study is much improved compared to that
360 introduced by Mouazen *et al.* (2007). This improvement can be attributed to the more accurate
361 model used in this study (Maleki *et al.*, 2006a) compared to that used by Mouazen *et al.* (2007).
362 The model of Maleki *et al.* (2006a) was built for only three soil textures, namely, loamy sand,
363 sandy loam and silt loam, whereas the model of Mouazen *et al.* (2007) was built for all texture
364 classes encountered in Flanders, the Northern part of Belgium. Furthermore, the model of
365 Maleki *et al.* (2006a) used more samples (204) for a smaller number of texture classes (3) as
366 compared to the smaller number of samples (175 samples) for a larger number of texture classes
367 used for the model of Mouazen *et al.* (2007). This makes the model developed by Maleki *et al.*
368 (2006a) more accurate than that developed by Mouazen *et al.* (2007) for prediction of P-avl for
369 these three texture classes. Since the texture of the Lovenjoel field (silt loam) is one of the three
370 textures valid for Maleki *et al.*, (2006a) model, it is logical that more accurate prediction has to
371 be achieved using this model (compared to the that of Mouazen *et al.* (2007)).

372 Comparing results given in Table 4 with those of Table 6, one can conclude that the
373 accuracy of on-line measurement of P-av1 (a smaller R^2 of 0.62, almost equal RMSE of 1.07 and
374 a smaller RPD of 1.42) is rather less than the off-line, non-mobile measurement (a larger R^2 of
375 0.68, almost equal RMSE of 1.08 and a higher RPD of 1.76). The reason of such degradation in
376 the accuracy of P-av1 prediction during on-line measurement is the deviation between the
377 starting point of a spectrum measurement as compared to that of corresponding soil sample
378 collected for laboratory chemical analysis. With the most accurate digital global positioning
379 system, a deviation in position of 0.5-1 m is expected. This deviation might introduce a source
380 of error, since the variability in soil is even smaller than this tolerance (1-0.5 m). Another reason
381 that might introduce a source of error is the larger surface (1.25 m) scanned by the
382 spectrophotometer compared to the amount of soil considered for the chemical analysis.

383

384 4. Conclusions

385

386 An approach to calibrate the tractor hydraulic system for successful on-line measurement of
387 soil spectra using visible and near infrared spectroscopy was introduced and tested. The
388 calibration included the determination of the optimal length of the tractor third point link (L)
389 and the manual adjustment of the hydraulic system to position the sensor at a specified depth,
390 while preserving a horizontal levelling of the sensor for maximum light reflection detection
391 from the bottom of the opened trench.

392 For successful on-line measurement, the soil-to-sensor distance (D) and angle (α) should be
393 minimised so that maximum electromagnetic energy reflected from the soil surface can be
394 collected. This also requires a successful mechanical design of the on-line sensor that ensures

395 continuous penetration into the soil, when it is set to the required depth after the proper
396 calibration of the tractor three-point linkage and hydraulic system is achieved. However, each
397 measurement depth requires a different calibration, which has to be carried out separately.

398 Modifying and correction of soil spectra is essential to improve the accuracy of on-line
399 measured soil properties. This becomes a critical step when on-line measurement is to be carried
400 out after root crops harvest (sugar beet or potato), since the soil layer penetrated by the sensor is
401 disturbed or even contains hollowed space. Therefore, the effect of correction of spectra would
402 have been greater if the crop had been a root crop instead of grass, since smaller variation in D
403 and α is experienced after grain crop harvest.

404

405 **Acknowledgements**

406

407 The authors acknowledge the IWT-Flanders (project nr: IWT/20711) for the financial
408 support.

409

410 **References**

411

412 Ben-Dor, E., Banin, A., 1995. Near-infrared analysis as a rapid method to simultaneously
413 evaluate several soil properties. *Soil Sci. Soc. Am. J.*, 59, 367-372.

414 Chang, C-W., Laird, D.A., Mausbach, M.J., Hurburgh, C.R., 2001. Near-infrared reflectance
415 spectroscopy-principal component regression analyses of soil properties. *Soil Sci. Soc. Am.*
416 *J.*, 65(2), 480-490.

- 417 Cohen, J., 1960. A coefficient of agreement for nominal scales. *Educ. Psychol. Measurement*.
418 20(1), 37-46.
- 419 Cozzolino, D., Morón, A. 2006. Potential of near-infrared reflectance spectroscopy and
420 chemometrics to predict soil organic carbon fractions, *Soil Tillage Res.*, 85(1-2), 78-85.
- 421 Dahm, D.J., Hahn, K.D., 2001. The physics of near-infrared scattering. In: Williams, P., Norris,
422 K. (Eds.), *Near-Infrared Technology in the Agriculture and Food Industries*. American
423 Association of Cereal Chemists, Inc. St. Paul, Minnesota, USA, pp. 1-17
- 424 Goovaerts, P., 1997. *Geostatistics for Natural Resources Evaluation*. Oxford University Press, New
425 York.
- 426 Landis, J.R., Koch, G.G., 1977. The measurement of observer agreement for categorical data.
427 *Biometrics*, 33, 159-174.
- 428 Maleki, M.R., Van Holm, L., Ramon, H., Merckx, R., De Baerdemaeker, J., Mouazen, A.M.,
429 2006a. Phosphorus sensing for fresh soils using visible and near infrared spectroscopy.
430 *Biosystems Engineering*, 95(3), 425-436.
- 431 Maleki, M.R., Mouazen, A.M., Ramon, H., De Baerdemaeker, J., 2006b. Optimisation of soil
432 VIS–NIR sensor-based variable rate application system of soil phosphorus. *Soil Tillage*
433 *Res.*, 94(1), 239-250.
- 434 Maleki, M.R., Mouazen, A.M., De Keterlaere, B., Ramon, H., De Baerdemaeker, J., 2007. On-
435 the-go variable rate phosphorus fertilisation based on a visible and near-infrared soil sensor.
436 *Biosystems Engineering*, 99(1), 35-46.
- 437 Maertens, K., Reyns, P., De Baerdemaeker, J., 2004. On-line measurement of
438 grain quality with NIR technology. *Transactions of the ASAE*, 47(4),
439 1135 - 1140

- 440 Mouazen, A.M., De Baerdemaeker, J., Ramon, H., 2005. Towards development of on-line soil
441 moisture content sensor using a fibre-type NIR spectrophotometer. *Soil Tillage Res.*, 80(1-
442 2), 171-183.
- 443 Mouazen, A.M., De Baerdemaeker, J., Ramon, H., 2006. Effect of wavelength range on the
444 measurement accuracy of some selected soil properties using visual-near infrared
445 spectroscopy. *Journal of Near Infrared Spectroscopy*, 14(3), 189-199.
- 446 Mouazen, A.M., Maleki, M.R., De Baerdemaeker, J., Ramon, H., 2007. On-line measurement
447 of some selected soil properties using a VIS-NIR sensor. *Soil Tillage Res.*, 93(1), 13-27.
- 448 Olsen, S.R., Cole, V.V., Watanabe, F.S., Dean, L.A., 1954. Estimation of
449 available phosphorus in soils by extraction with sodium bicarbonate.
450 U.S. Department. of Agricultural Circular, 939, Washington, DC.
- 451 Odlare, M., Svensson, K., Pell, M., 2005. Near infrared reflectance spectroscopy for assessment
452 of spatial soil variation in an agricultural field. *Geoderma*, 126(3-4), 193-202.
- 453 Pannatier, Y. 1996. *Variowin*. Springer, New York.
- 454 Reeves, J.B., McCarty, G.W., 2001. The potential of near infrared reflectance spectroscopy as a
455 tool for spatial mapping of soil composition for use in precision agriculture. *Journal of*
456 *Near Infrared Spectroscopy*, 9(1), 25-34.
- 457 Reynolds, P., Maertens, K., De Baerdemaeker J., 2001. On-line measurement of corn moisture
458 content on a combine harvester using NIR technology. In: Grenier, G., Blackmore, S.,
459 (Eds.), *Proceedings of the 3rd European Conference on Precision Agriculture*. Agro
460 Montpellier, Montpellier, France pp. 851-856.
- 461 Shibusawa, S., I made Anom, S.W., Hache, C., Sasao, A., Hirako, S., 2003. Site-specific crop
462 response to temporal trend of soil variability determined by the real-time soil

463 spectrofotometer. In: Stafford J.V. (Ed), Proceedings of the Joint European Conference of
464 ECPA-ECPLF, Wageningen Academic Publishers, Berlin, Germany, pp. 639-643.

465 Shonk, J.L., Gaultney, L.D., Schultze, D.G., Van Scoyoc, G.E. 1991. Spectroscopic sensing of
466 soil organic matter content. Transactions of the ASAE, 34(5), 1978-1984.

467 Sudduth, K.A., Hummel, J.W., 1993. Soil organic matter, CEC, and moisture sensing with a
468 prototype NIR spectrophotometer. Transactions of the ASAE, 36(6), 1571-1582.

469 Wetterlind, J., Stenberg, B., Jonsson, A., 2008. Near infrared reflectance spectroscopy
470 compared with soil clay and organic matter content for estimating within-field variation in N
471 uptake in cereals. Plant and Soil, 302(1-2), 317-327.

472

473

474

475

476

477

478

479

480

481

482

483

484

485

486

487

488

Tables

489

490 Table 1.

491 Soil texture fraction of the experimental field topsoil (0-20 cm) according to the USDA Soil
 492 texture classification

493

Particle size	Heverlee field	Lovenjoel field
	silt loam	silt loam
Sand (> 50 μm) (g kg^{-1})	90	202
Silt (2 – 50 μm) (g kg^{-1})	778	697
Clay (< 2 μm) (g kg^{-1})	132	101

494

495

496

497

498

499

500

501

502

503

504

505

506

507

508

509 Table 2

510 Soil moisture content measured at 15 cm depth and calculated soil-to-sensor distance and angle

511 α in both experimental fields

	Third point link length (L) (mm)	Soil-to-sensor distance (D) (mm)	Soil-to-angle angle (α) (deg)	Average soil moisture content (kg kg⁻¹)
<i>Heverlee field</i>				
Line A	545	6	0.6	20.1
Line B	550	3	0.3	19.4
Line C	555	0.0	0.0	19.2
Line D	560	0.0	-0.2	18.7
Line E	565	0.0	-0.6	19.4
<i>Lovenjoel field</i>				
All field lines	562	0.0	-0.42	16.1

512

513

514

515

516

517

518

519

520

521

522 Table 3.

523

524 Chemical analysis results of plant available phosphorus (Olson method) in soil for 126 samples
525 of Lovenjoel field

526

	No.	Maximum	Minimum	Mean	Standard deviation
Available phosphorus (mg 100g ⁻¹)	126	11.0	2.9	4.8	1.7

527

528

529

530

531

532

533

534

535

536

537

538

539

540

541

542

543 Table 4.

544 Statistics results of Partial Least Squares (PLS) model of plant available phosphorus in soil (P-

545 avl) resulted from samples collected from many fields of Belgium having texture classes of

546 loamy sand, sandy loam and silt loam (Maleki *et al.*, 2006a)

547

Statistics	Sub-set samples		
	Calibration	Full cross validation	Laboratory validation on off-line spectra
R ²	0.83	0.73	0.68
Slope	0.83	0.76	1.007
Offset	1.219	1.71	-0.709
RMSE (mg 100g ⁻¹)	0.943	1.202	1.08
Bias (mg 100g ⁻¹)	-6.3 × 10 ⁻⁷	0.01157	0.67
RPD	-	1.92	1.76
RER	-	7.22	7.72

548 RMSE, root mean square error
549 R², coefficient of determination
550 RPD, ratio of prediction deviations
551 RER, ratio error range

552

553

554

555

556

557

558

559 Table 5.

560 Statistics about on-line collected soil spectra (8 spectra) in Heverlee field at different length of

561 the tractor third point link (L)

562

Line	Length of third point link (L) (mm)	Number of successful spectra	Percentage of successful spectra (%)	Average maximum reflectance (AMR) (%)
A	545	1	12.5	7.79
B	550	4	50.0	30.60
C	555	8	100.0	75.68
D	560	8	100.0	43.28
E	565	8	100.0	33.15

563

564

565

566

567

568

569

570

571

572

573

574

575 Table 6.

576 Statistics results of plant available phosphorus in soil (P-avl) prediction using on-line measured

577 spectra in Lovenjoel field

578

<i>Statistics</i>	<i>Sub-set samples</i>	
	Raw uncorrected spectra	Corrected spectra
R ²	0.56	0.62
Slope	0.7231	0.7079
Offset	1.4822	1.5134
RMSE (mg 100g ⁻¹)	1.15	1.07
Bias (mg 100g ⁻¹)	-0.139	-0.128
RPD	1.39	1.42
RER	6.47	6.71

579

RMSE, root mean square error

580

R², coefficient of determination

581

RPD, ratio of prediction deviations

582

RER, ratio error range

583

584

585

586

587

588

589

590

591

592

593 **Figure captions**

594

595 Fig. 1. The optical probe attached to the backside of the penetration tine

596

597 Fig. 2. Optical path throughout the optical probe for (a) tine at optimal position (b) tine inclined
598 backward (c) tine inclined forward

599

600 Fig.3. Recorded soil spectra at different probe inclination angle (α) resulted from different
601 lengths of the tractor third-point link (L); (a) $\alpha = 0.6^\circ$ at L = 545 mm; (b) $\alpha = 0.3^\circ$ at L = 550
602 mm; (c) $\alpha = 0.0^\circ$ at L = 555 mm; (d) $\alpha = -0.2^\circ$ at L = 558 mm; (e) $\alpha = -0.6^\circ$ at L = 565 mm

603

604 Fig. 4. Soil sampling locations in a grid of 6 by 10 m in a 100 by 200 m Lovenjoel field

605

606 Fig. 5. Corrected spectra measured for line C in Heverlee field with 555 mm long third point
607 link (L)

608

609 Fig. 6. Standardised variograms of plant available phosphorus in soil (P-avl) based on laboratory
610 chemical analysis, uncorrected and corrected on-line measured soil spectra in Lovenjoel field

611

612 Fig. 7. A 1 by 1 m grid obtained by ordinary kriging of plant available phosphorus in soil (P-
613 avl) based on: (a) laboratory chemical analysis, (b) uncorrected, and (c) corrected on-line
614 measured soil spectra in Lovenjoel field

615

616 Fig. 8. Categorical maps of plant available phosphorus in soil (P-avl) based on (a) laboratory
617 chemical analysis, (b) uncorrected, and (c) corrected on-line measured soil spectra in Lovenjoel
618 field

619

620

621

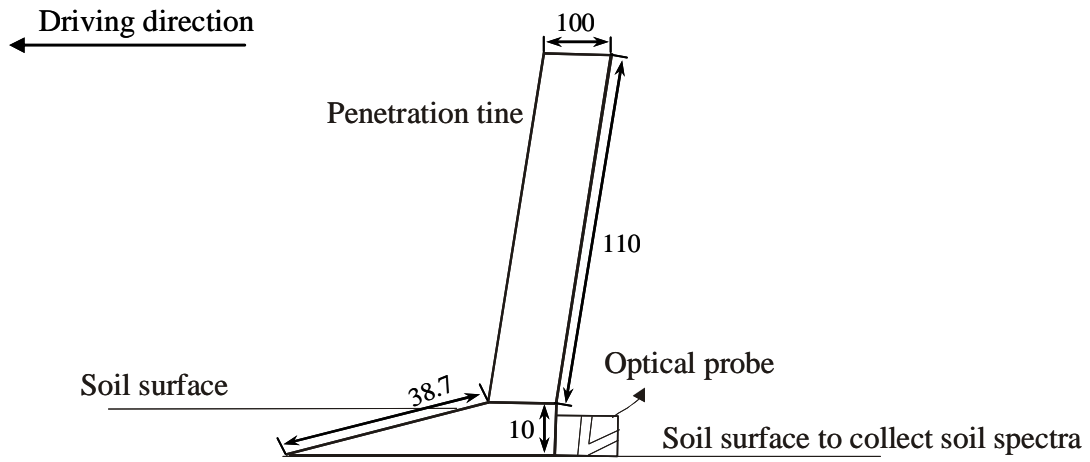


Fig. 1. The optical probe attached to the backside of the penetration tine

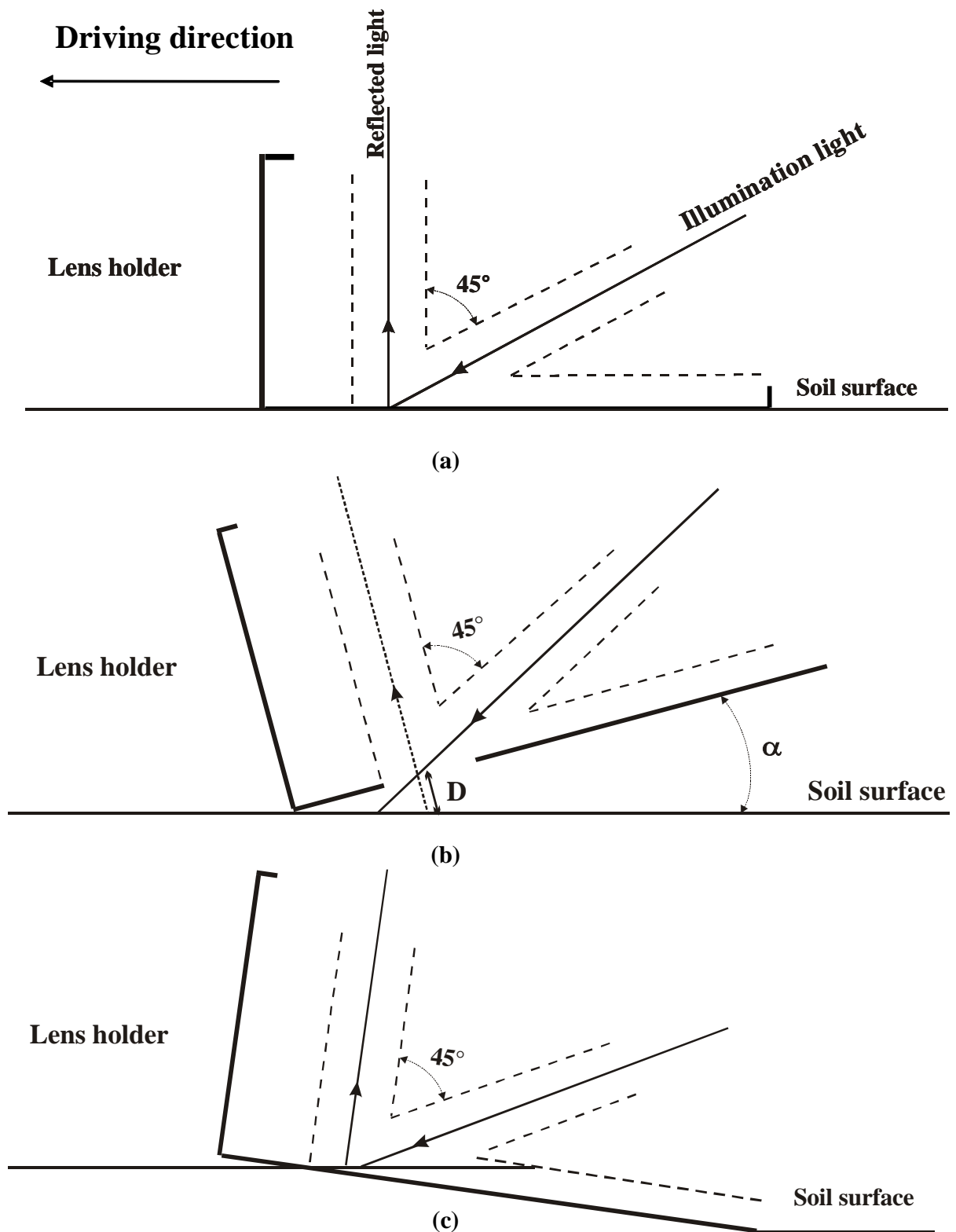
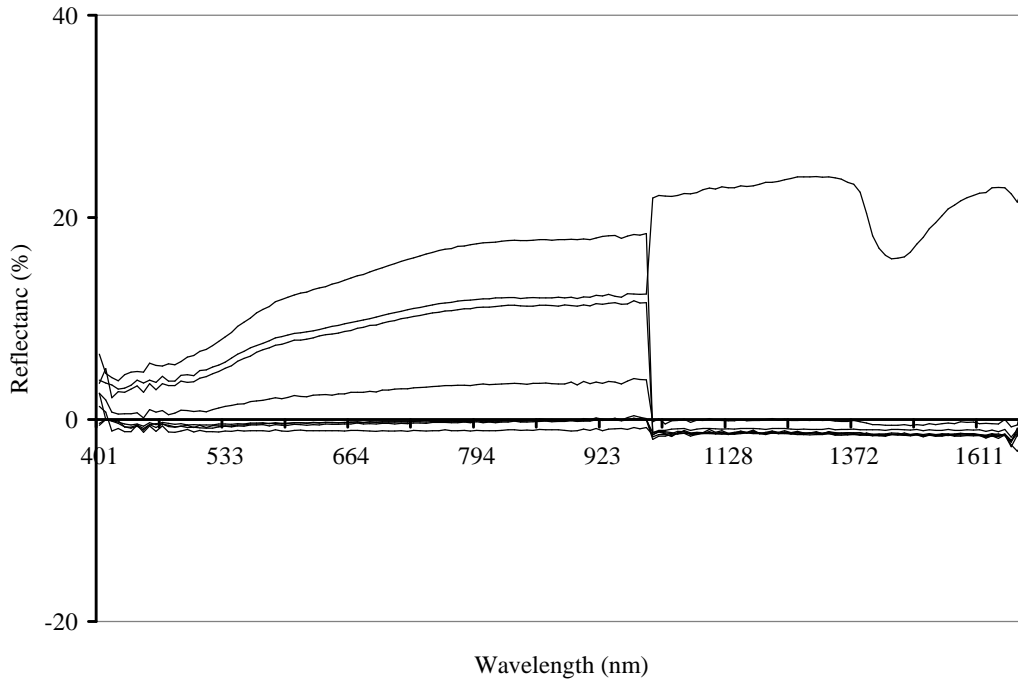
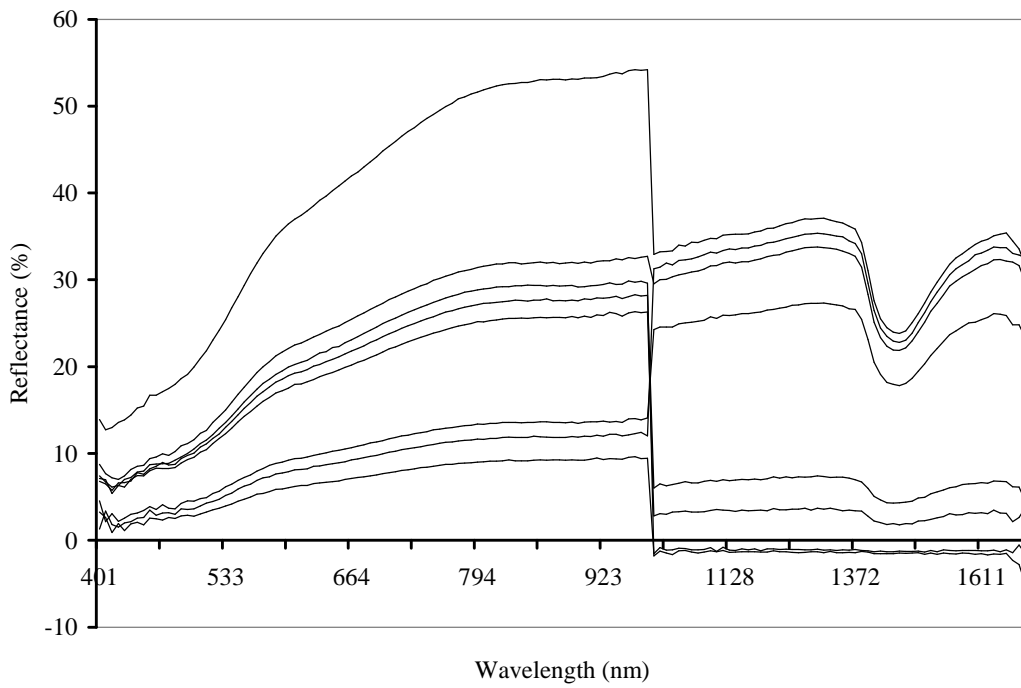


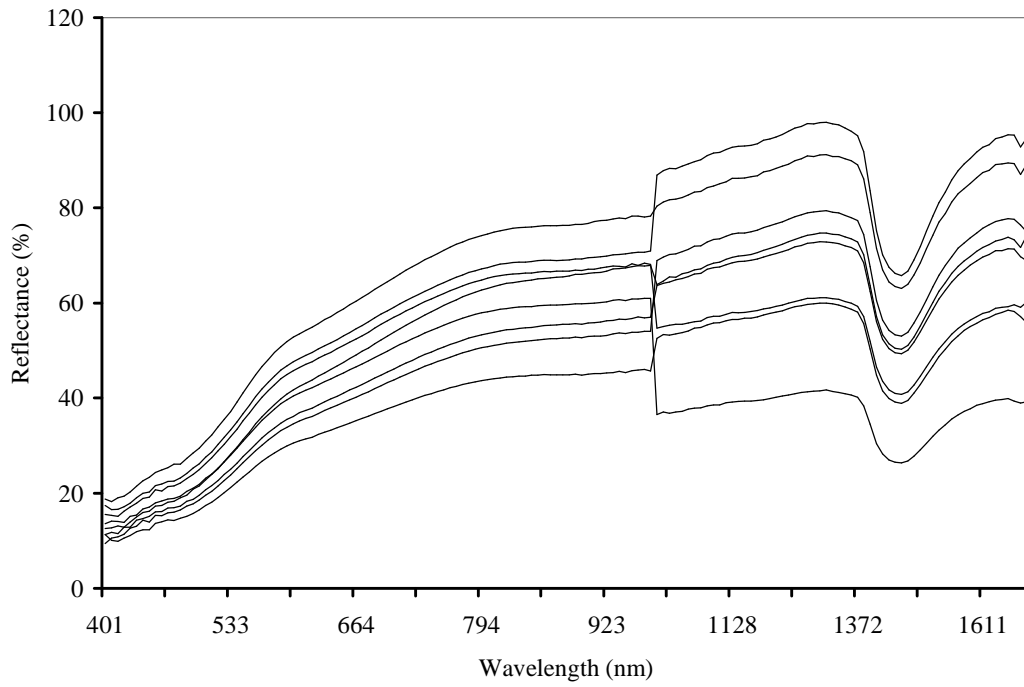
Fig. 2. Optical path throughout the optical probe for (a) tine at optimal position (b) tine inclined backward (c) tine inclined forward



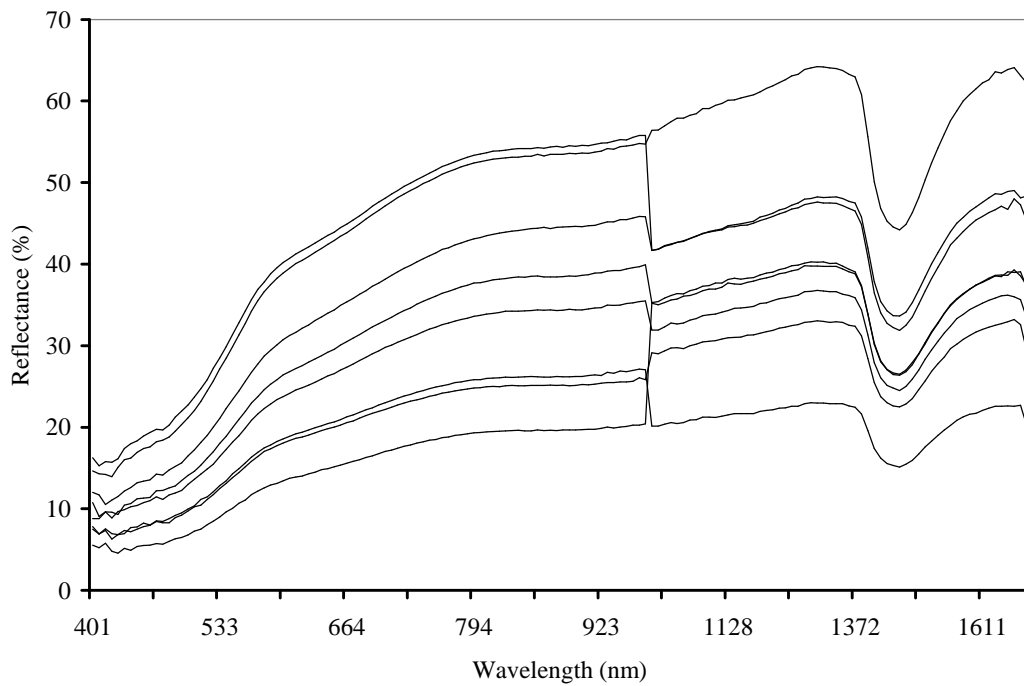
(a)



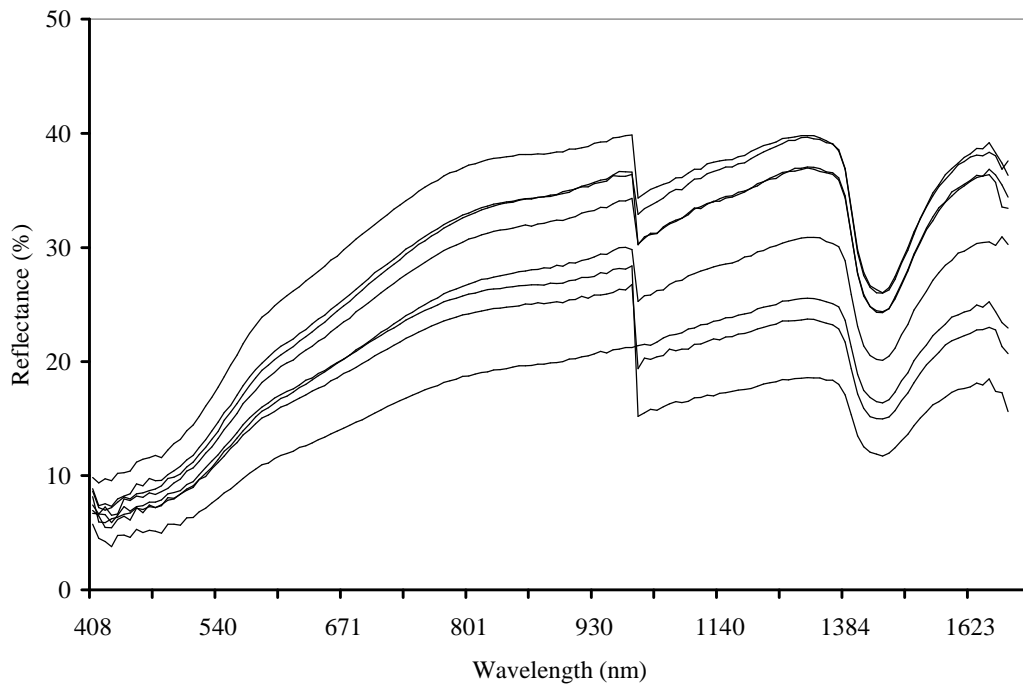
(b)



(c)



(d)



(e)

Fig.3. Recorded soil spectra at different probe inclination angles (α) resulted from different lengths of the tractor third-point link (L); (a) $\alpha = 0.6^\circ$ at $L = 545$ mm; (b) $\alpha = 0.3^\circ$ at $L = 550$ mm; (c) $\alpha = 0.0^\circ$ at $L = 555$ mm; (d) $\alpha = -0.2^\circ$ at $L = 558$ mm; (e) $\alpha = -0.6^\circ$ at $L = 565$ mm

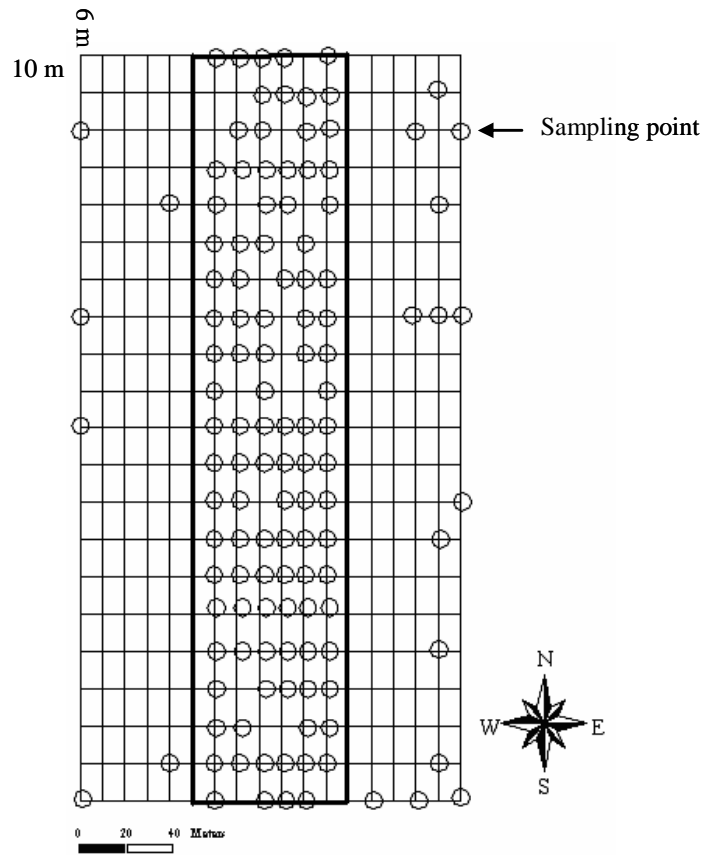


Fig. 4. Soil sampling locations in a grid of 6 by 10 m in a 100 by 200 m Lovenjoel field

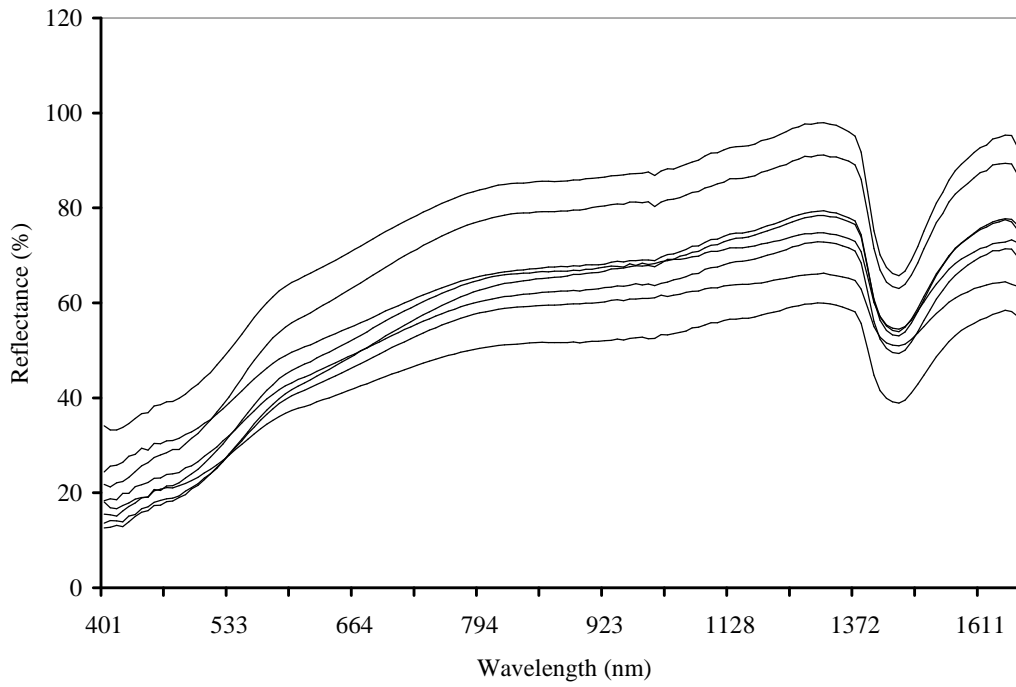


Fig. 5. Corrected spectra measured for line C in Heverlee field with 555 mm long third point link (L)

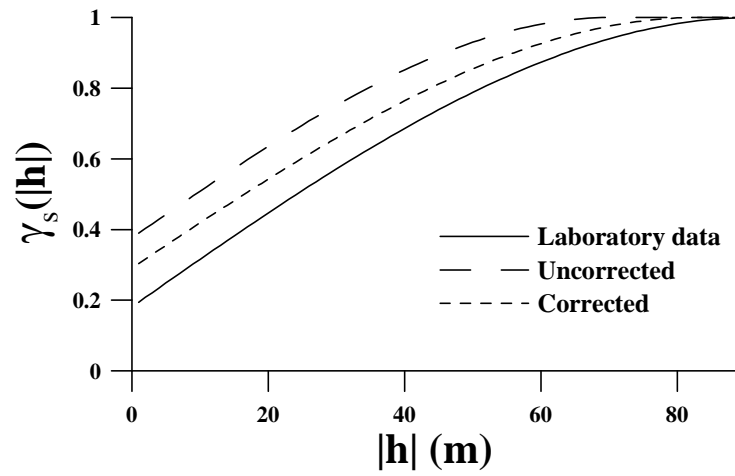
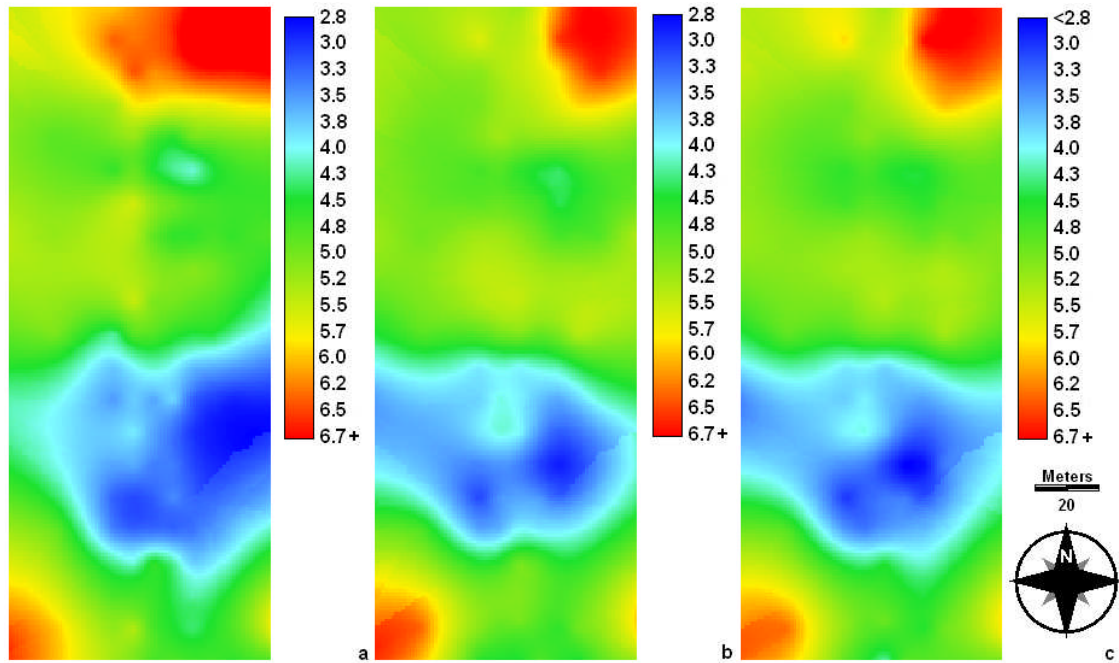


Fig. 6. Standardised variograms of *plant available phosphorus in soil (P-avl)* based on laboratory chemical analysis, uncorrected and corrected on-line measured soil spectra in Lovenjoel field



*Fig. 7. A 1 by 1 m grid obtained by ordinary kriging of **plant available phosphorus in soil** (P-avl) based on: (a) laboratory chemical analysis, (b) uncorrected, and (c) corrected on-line measured soil spectra in Lovenjoel field*

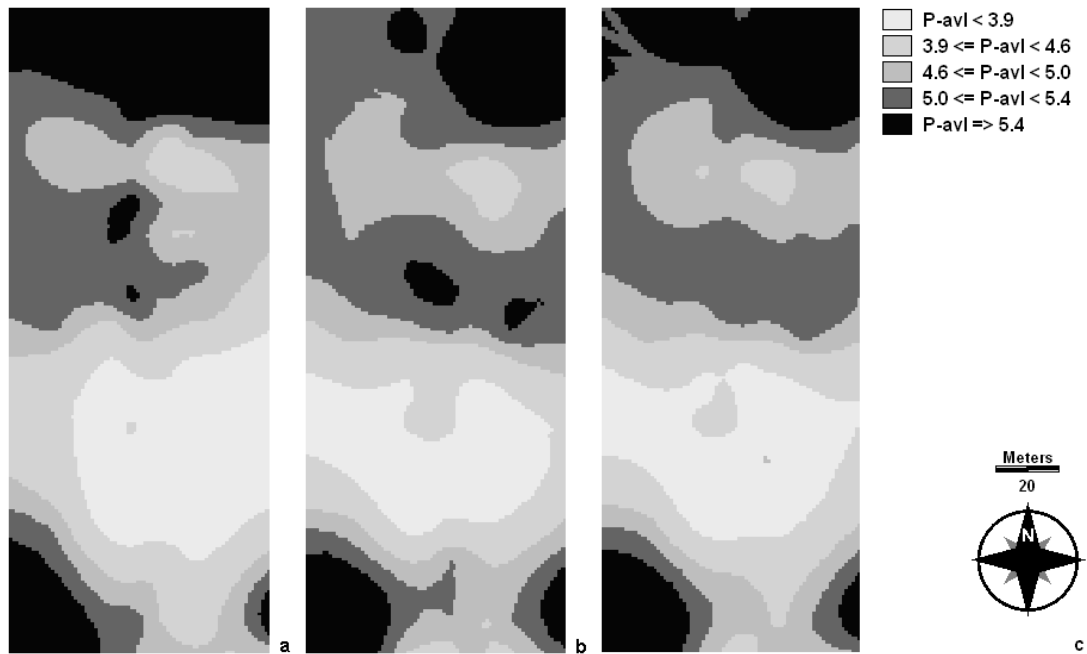


Fig. 8. Categorical maps of *plant available phosphorus in soil* (P-avl) based on (a) laboratory chemical analysis, (b) uncorrected, and (c) corrected on-line measured soil spectra in Lovenjoel field